Comparing Experimental and Numerical Results for the Structural Properties of Lightweight Ferrocement Beams with Different Core Materials

Abstract:

The main objective of this research is comparing experimental and numerical results for the structural properties of lightweight Ferrocement beams with different core materials. Additionally, look into the potential of using lightweight materials for the core with the goal of creating a system that is both ecologically friendly and has a light weight. The experimental program involved casting and testing eleven 200x100x2000mm reinforced concrete beams. These beams are divided into four groups, with about three beams in each group. In all groups, use standard formwork. The beams in this group 1 were reinforced with two steel bars of 10 mm diameter at the top and12mm diameter bottom of the beams. The beams in the other three groups, on the other hand, were cast using Ferrocement beams. Two steel bars with a 10 mm and 12 mm diameter each were placed at the top and bottom of these beams to reinforce the core. Expanded steel mesh and welded wire mesh, two forms of steel mesh used to support ferrocement beams, were studied. We looked at single mesh and two layers made of mesh and a strip steel mesh. Light brick, foam, and lightweight concrete were the three types of core materials that were examined. The test specimens were put through a simple beam test with a three-point loading scenario across an 1800 mm span. The performance of the test beams in terms of strength, cracking behavior, ductility, and energy absorption properties was investigated. The behavior of the developed beams was compared to that of the control beams. Experimental results were then compared to analytical models using (ABAQUS/ CEA) programs. The results showed that the type of reinforcement affects the ductility ratio, ultimate strength and energy absorption properties of the beams Comparison between the experimental results and the results obtained from both the theoretical model as well as the finite element one showed that there is a close agreement for all beams. This agreement verified the validity of these models.

Keywords: ferrocement; composite material; expanded steel mesh, welded wire mesh experimental study, ABAQUS/CEA.

1.INTRODUCTION

A type of reinforced concrete called ferrocement differs from conventional reinforced or prestressed concrete primarily in how the reinforcing components are distributed and arranged. It is constructed of numerous layers of fine rods or mesh that are fully enmeshed in cement mortar.

According to the test results, hollow beams with size reductions of 16 and 28.4 percent had ductility that was higher than that of the reference solid beam, while hollow beams with a size reduction of 44.4 percent had ductility that was equal to that of the solid beam.

An experimental investigation was used to

Ferrocement is a building material that has clear advantages for thin-walled components. For curves and folded thin elements with rigidity attributable to the form rather than the quantity of material due to its qualities, ferro cement is advised. A promising approach is the use of ferrocement to increase the flexural strength of damaged reinforced concrete.

Sometimes pre-cast concrete slabs with voids are used to reduce self-weight and manufacturing expenses; these slabs are known in the industry as hollow core slabs. It is frequently used in industrial and residential buildings due to its appealing benefits, including high quality, ease of installation, high thermal and acoustic insulation, superior fire resistance, earthquake resilience, and the ability to provide longer spans than standard solid slabs [1].

The improvement of the ductile behavior of ferrocement I-beams has been attempted in many ways, as shown by [2], in order to boost their practical utility. The calculation of the theoretical analysis in comparison to the actual flexural strength of the reinforced concrete I-beam with additional layers of wire mesh in the flange section.

The ferrocement channels were designed and built using a variety of materials. Additionally, a suitable mesh combination was discovered using ABAQUS Unified FEA, and channels finite element FE models were produced [3].

Sandwich panels were created by Ferrocement as a result of research into the structural behavior of light-weight cement walls and for use as wall-bearing components. The proposed panels are less in weight than conventional reinforced concrete panels [4] [5].

[6] investigated the flexural behavior of hollow high-strength concrete beams as their size was decreased.

examine how different types of reinforcement affected the flexural behavior of thin hollow core slabs made of cement with embedded PVC pipes [7].

The slab reinforced with steel bars had the lowest deflection and the highest rigidity of all the slabs tested, whereas the slab reinforced with only macro steel fibers had the highest flexural strength.[8] We out an experimental study on the flexural behavior of hollow core concrete slabs. According to the study.

2.MATERIALS

• **The fine aggregate**: It satisfies ASTM C136-84a specifications in terms of quality. It was essentially pure and clean, with a specific gravity of 2.65 t/m3 and a fineness modulus of 2.55. [9].

• **The coarse aggregate**: utilized had a specific gravity of 2.75 t/m3, a crushing modulus of 18.5%, and an absorption of 2.1%, all of which met the standards of the Egyptian Code 203/2007. [10].

• **Super plasticizer:** One kind of chemical admixtures is employed as a super plasticizer. As a plasticizer, a high range water reducer (HRWR) that satisfies ASTM C494 (type A and F) standards is employed (trade name: Master Glenium RMC 315). Superplasticizers are employed in the production of high-quality concrete. [11].

• **Silica fume (S.F.):** utilized to increase the durability of the cement mortar and concrete core. It was used as a partly weight-for-weight replacement for cement in mortar compositions.[12].

• **The cement:** manufactured by the Al-Amreya cement mill, Ordinary Portland cement was utilized.

• **Fly ash:** used in small amounts to manufacture cement. It meets with the relevant ASTM C618 chemical and physical

requirements as well as the applicable international quality criteria for fly ash [13].

• **Water:** In order to combine and cure the R.C. beams that were put through E.C.P. 203/2007 testing, pollutant-free, pure fresh

3.1 CONCRETE MITXTURE

In order to boost mortar matrix strength without significantly affecting the mix's quality and characteristics in both the fresh and hardened phases, the main goal of mix de-

water was used.

• **Fine Expanded Perlite:** Light Weight Concrete is also known as Light Density Concrete, according to ACI. It is defined as concrete made from lightweight coarse aggregate, heavyweight fine aggregate, and possibly some lightweight fine aggregate.[14].

• **Light brick:** A 400x200x70 mm light weight brick that is produced commercially [15].

• **Foam:** The thermal insulation boards sold under the brand name Advefoam comply with ASTM C578 standards. [16].

• **Reinforcing steel:** 12 mm-diameter high tensile steel bars have undergone deformation. Similar to this, control beams and the concrete core of the test specimens built of ferrocement beams were reinforced with high tension steel bars with a 10 mm diameter.

• **Expanded steel mesh.**

• **Welded wire mesh.**

3. TESTING PROGRAM

The goal of this research's experimental program was to test the viability and efficiency of creating structural cement beam forms filled with various types of core material as a feasible replacement for traditional reinforced concrete beams. To investigate the impact of these test parameters on the strength, stiffness, cracking behavior, ductility, and energy absorption of the tested concrete beams incorporating permanent ferrocement forms, the current experimental program varied the type and number of reinforcement steel. Two types of steel mesh reinforcement were used These types are: welded wire mesh, and expanded steel mesh. Single and double layers of each type were used. Three types of core material were utilized. These types are: light brick core, foam core and light weight concrete admixed with perlite as shown in Table(1), along with the details of the experimental program of all the test specimens. Fig. (1) also reveals all the details of reinforcement for all specimens.[17]

sign was to ascertain how a significant proportion of cement might be partially replaced by fly ash and silica fume. The mortar matrix's capacity to work through the steel mesh reinforcing layers was crucial. Table (2) shows proportions by weight of the normal concrete mix.

To improve the flow properties and hasten the onset of strength, a hyper plasticizing chemical was utilized. At a ratio of 0.35 water to cement and 1.5% by weight of cement, super plasticizer is utilized.

Perlite was used as a replacement for aggregate in the control concrete at a mass ratio of 30%, giving it a compressive strength of 39 MPa (w/c = 0.35) instead of aggregate. Perlite-containing concrete has a 20 MPa compressive strength. The light weight concrete and perlite mix proportions, measured in weight. [17].

3.2 Preparation of Test Specimens

The mold is made of contras wood and has a base plate that **is 22**00x600x9mm. Before the mold was disassembled, the ferrocement forms were allowed to sit in the mold for 24 hours site of the load application. Two strain gauges are positioned two centimeters from the top and bottom edges. Three testing lines were run through all beams. The linear variable of the test beam's midspan.[17]

Table (1) The Details of the Test Specimens.[17]

Group	Specimens Designation	Specimen's Core	Reinforcement details			No. of Layer	Type of Mesh
			Tension Steel bars	Tension Steel bars	Stirrups		
A	A1	———	2 Φ 12	2 Φ 10	Φ6@150mm	———	———
	A2	———	2 Φ 12	2 Φ 10	Φ6@150mm	———	———
B	B1	Light Brick	2 Φ 12	2 Φ 10	———	1	Welded Wire Mesh
	B2	Light Brick	2 Φ 12	2 Φ 10	———	2	Welded Wire Mesh
	B3	Light Brick	2 Φ 12	2 Φ 10	———	2	Expanded steel Mesh
G	G1	Foam	2 Φ 12	2 Φ 10	———	1	Welded Wire Mesh
	G2	Foam	2 Φ 12	2 Φ 10	———	2	Welded Wire Mesh
	G3	Foam	2 Φ 12	2 Φ 10	———	2	Expanded steel Mesh
F	F1	Perlite	2 Φ 12	2 Φ 10	———	1	Welded Wire Mesh
	F2	Perlite	2 Φ 12	2 Φ 10	———	2	Welded Wire Mesh
	F3	Perlite	2 Φ 12	2 Φ 10	———	2	Expanded steel Mesh

Table (2) Proportions by Weight of the Normal Concrete Mix.[17]

Material	Cement	Sand	Coarse Aggregates	Water	Silica fume	Superplasticizer	Fly ash
Weight (kg/m^3)	340	680	1360	119	51	5.1	68

Normal Weight Concrete. A1 Ferrocement Concrete.A2

a) Group (A**)**

B1	**B2**	**B3**

b) Group (B).

G1	**G2**	**G3**

c) Group (G).

F1	**F2**	**F3**

d) **Group (F).**

Fig. (1): Cross Sections of the Tested Beams.[17].

4.FINITE ELEMENT SIMULATION

4.1 PARTS MODELING

The specimens of study were modeled as 3D structures in Abaqus. Concrete parts were modeled using C3D8R.

Steel bars, welded and expanded steel mesh were modeled using T3D2 elements. Fig. (2) shows modeling of all parts in ABAQUS/CEA.[18]

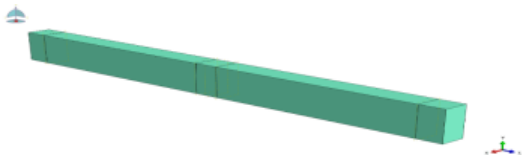

a) Modeling of Concrete Beam.

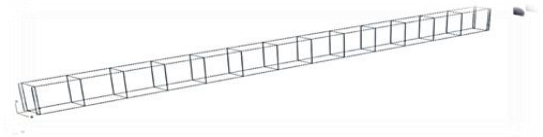

b) Modeling of Steel Bars and Stirrups.

c) Modeling of Expanded Steel Mesh.

d) Modeling of Welded Wire Mesh.

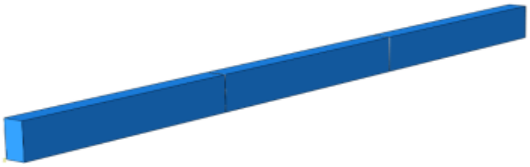

e) Modeling of Light bricks.

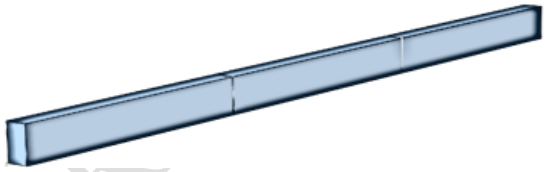

f) Modeling of Light bricks

Fig. (2): Modeling of all parts in ABAQUS/CEA.

4.2 MATERIALS MODELING

4.2.1 CONCRETE

Concrete material was modeled using Abaqus concrete damage plasticity model. This model uses the concept of isotropic damage elasticity in combination with isotropic compression and tensile plasticity to model the inelastic behavior of concrete. Tables (3) and (4) present concrete elastic properties and concrete damaged plasticity model parameter used in analysis.

4.2.2 STEEL REINFORCEMENT AND METAL MESHES

Steel reinforcement has approximately linear elastic behavior when the steel stiffness introduced by the Young's or elastic modulus keeps constant at low strain magnitudes. At higher strain magnitudes, it begins to have nonlinear, inelastic behavior, which is referred to as plasticity. The plastic behavior of steel is described by its yield point and its post-yield hardening. The shift from elastic to plastic behavior occurs at a yield point on a material stress-strain curve. Table (5) shows the elastic properties of steel bars and metal mesh.

Table (3) Elastic Properties of Concrete.

Parameter	Model (1) (Ordinary Concrete)	Model (2) (Ferrocement)
Mass density, kg/m3	2200	2200
Modulus of elasticity (Es)	22131.6 MPa	32393.1MPa
Poisson's ratio (υ)	0.19	0.21

Table (4) Concrete Damaged Plasticity Parameters

Parameter	Dilation angle	Eccentricity	fb0/fc0	K	Viscosity p.
Model (1) (Ordinary Concrete)	39	0.11	1.36	0.67	0.000001
Model (2) (Ferrocement)	41	0.12	1.36	0.67	0.000001

Table (5) Elastic Properties of Steel Bars and Metal Meshes.

Steel 24/35		**Steel 36/52**		**Expended Mesh**		**Welded Mesh**	
Density (t/m3)		**Density (t/m3)**		**Density (t/m3)**		**Density (t/m3)**	
7.86		7.86		7.86		7.86	
E	**Poisson's ratio**	**E**	**Poisson's ratio**	**E**	**Poisson's ratio**	**E**	**Poisson's ratio**
205000	0.3	210000	0.3	130000	0.28	170000	0.28
Stress	**Strain**	**Stress**	**Strain**	**Stress**	**Strain**	**Stress**	**Strain**
240	0	570	0	199	0	413	0
350	0.0951	730	0.0831	320	4.95E-02	610	0.05763

4.3 INTERACTION

Steel bars and metal meshes are modeled as embedded regions in the surrounding solid elements in the beams shown in Fig. (3).

4.4 BOUNDARY CONDITION

In Abaqus model tree, boundary condition can be added using *Load option and choosing *Create boundary condition. A fixation was made for the two steel parts that represent rollers supports in all directions and relying on interaction between concrete beam and rollers surface to reach the closest possible behavior to experimented samples as shown in Fig. (4).

Also, rigid steel circular plate which represents loading plate was prevented from translation and rotation in all direction except translation in Z-direction to apply load correctly as shown in Fig. (5).

4.5 MESHING OF MODEL

In current models, concrete beam had a size of mesh (10×10×10) mm, in all cores had a size of mesh (20×20×20) mm Truss element

4.6 COMPARSION BETWEEN EXPERIMENTAL AND FINITE ELEMET METHOD RESULT

The comparison between experimental and Finite Element Method results ultimate load, 1st crack load, mid span deflection at the ultimate load are illustrated in table (6). Fig. (7) and Fig. (8) present the applied load-mid span deflection, and the applied load-strain curves; respectively as obtained from the experimental and theoretical results for the all beams tested. The first crack load was determined as the first deviation from linearity of load deflection curve. The comparison between the experimental and theoretical cracking patterns for all tested specimens is presented in Fig. (6). Stresses distribution for all beams tested can be obtained at Fig. (10). Consequently, it can be concluded that the Finite Element Method give accurate results in comparing with the experimental results. In addition, these comparisons indicate a good agreement in slope of curves in the linear stage. For nonlinear stage, and due to the possibility of the inaccuracy in

of steel reinforcement had a size of 20 mm. The expanded steel mesh had a size of 30 mm and welded wire mesh mesh had a size of 15 mm were shown in Fig. (6).

modeling the post yield behaviour of steel rebar material, there is somewhat none agreement between the finite element results and those of experimental results

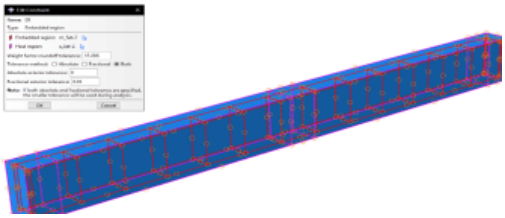

Fig. (3). Embedded Region Interaction.

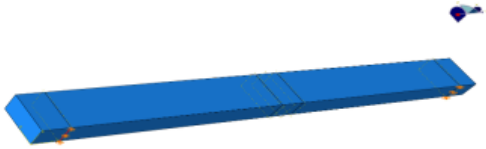

Fig. (4). Simply Supported Boundary Condition of Model.

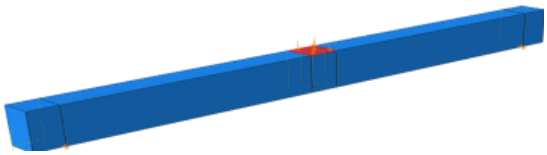

Fig. (5). Boundary Condition of Loading Plate.

Fig. (6). Mesh Configuration of Finite Element Model

Table (6) A Comparison Between the Experimental and Theoretical Results.

Specimens Designation	Specimen No.	Initial Crack Load (k.N)			Ultimate Load (k.N)			Deflection (mm)		
		Finite Element Meth Results	Experimental Study Results	Percentage of Difference	Finite Element Meth Results	Experimental Study Results	Percentage of Difference	Finite Element Meth Results	Experimental Study Results	Percentage of Difference
A	**A1**	6.63	7.084	6.4	43.62	44.212	1.33	8.34	8.47	1.54
	A2	9.976	10.66	6.42	48.17	49.874	3.42	7.996	8.18	2.25
B	**B1**	9.174	9.657	5.0	40.63	41.689	2.54	8.032	7.82	2.71
	B2	11.19	10.32	8.43	47.95	46.986	2.05	9.306	9.6	3.06
	B3	12.37	13.99	11.58	57.61	56.232	2.45	9.66	10.00	3.40
G	**G1**	9.257	11.62	20.33	38.23	37.932	0.79	7.766	8.69	10.6
	G2	10.66	12.85	17.04	44.06	44.785	1.62	9.551	10.19	6.27
	G3	11.86	13.50	12.14	52.46	52.941	0.91	9.794	10.33	5.19
F	**F1**	11.77	14.21	17.17	51.99	53.488	2.80	11.29	11.57	2.42
	F2	13.26	15.57	14.83	55.27	55.688	0.75	12.12	12.32	1.62
	F3	14.06	16.0	6.41	61.98	62.786	1.28	12.70	12.57	1.03

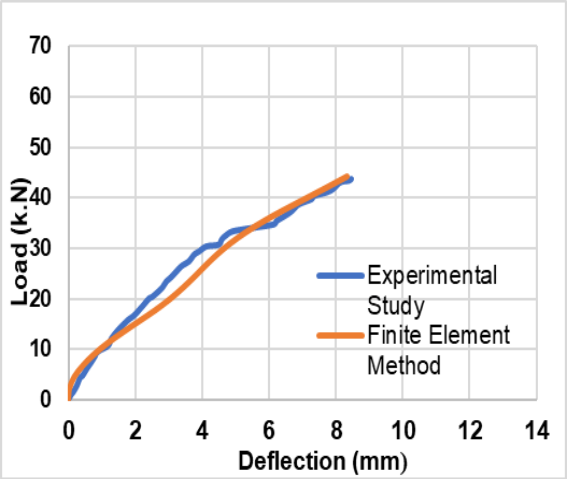

a) **Load-Deflection Curves for Beam (A1).**

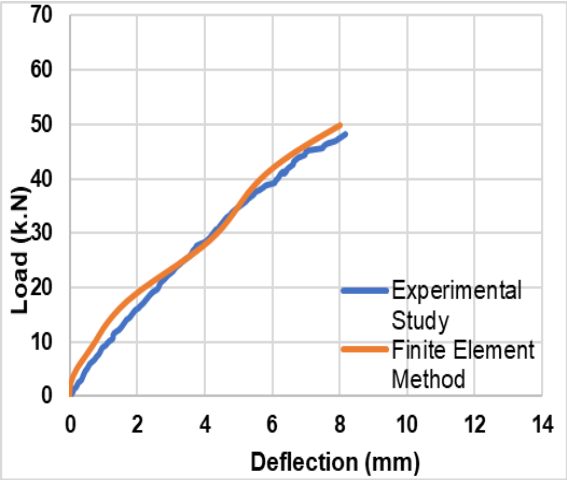

b) **Load-Deflection Curves for Beam (A2).**

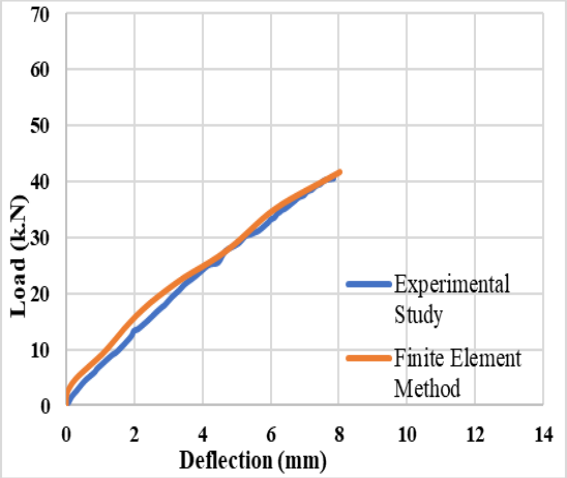

c) **Load-Deflection Curves for Beam (B1).**

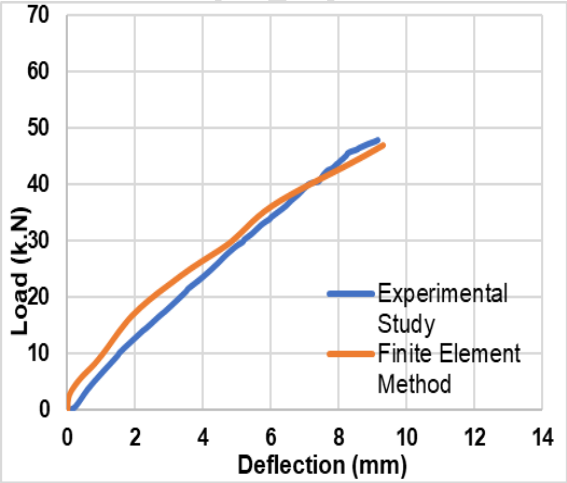

d) **Load-Deflection Curves for Beam (B2).**

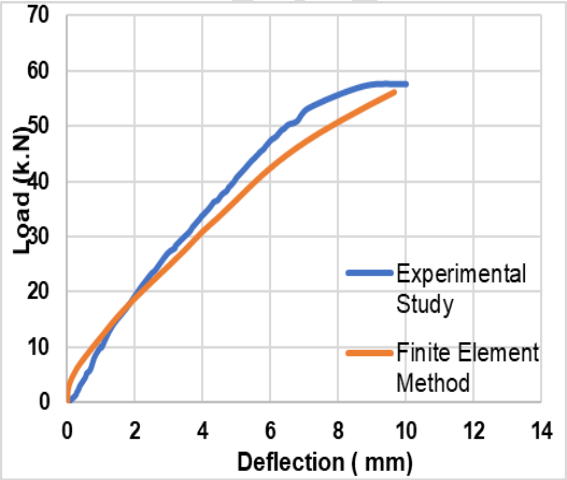

e) **Load-Deflection Curves for Beam (B3).**

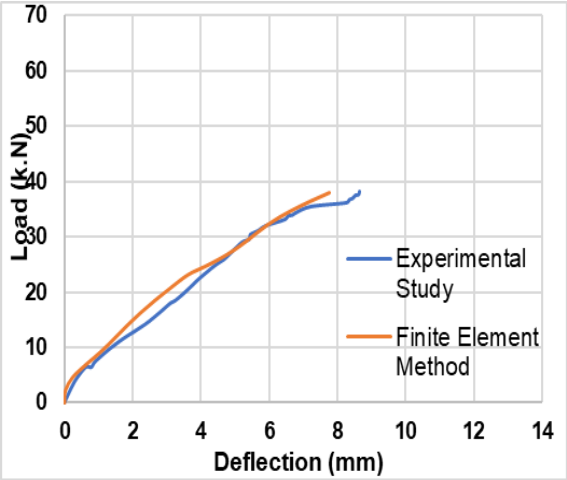

f) **Load-Deflection Curves for Beam (G1).**

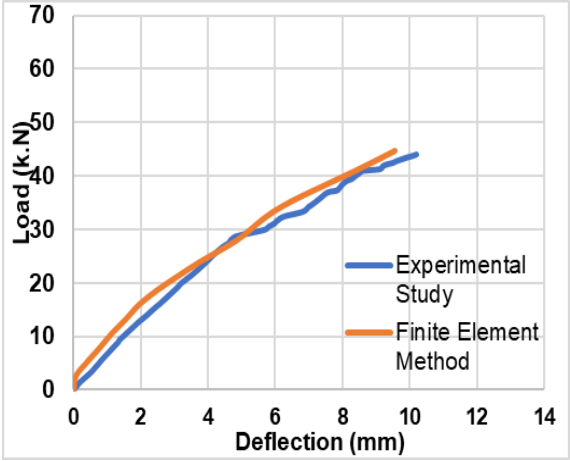

g) Load-Deflection Curves for Beam (G2).

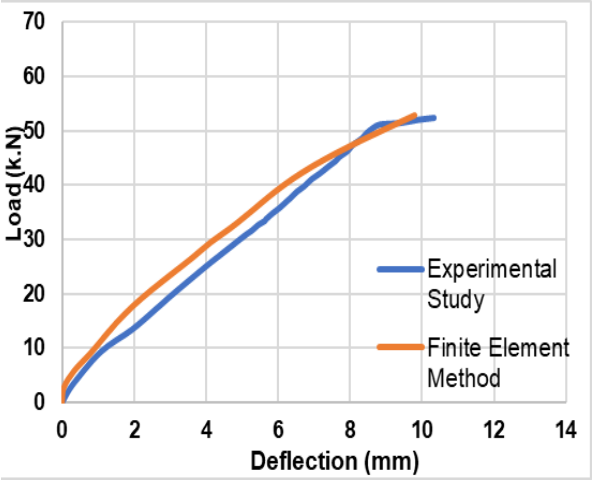

h) Load-Deflection Curves for Beam (G3).

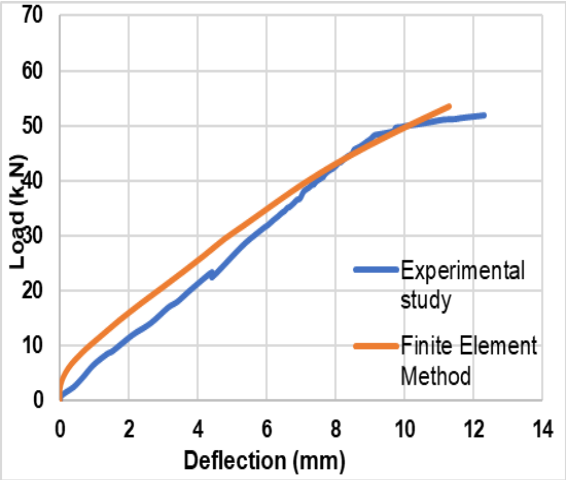

i) Load-Deflection Curves for Beam (F1).

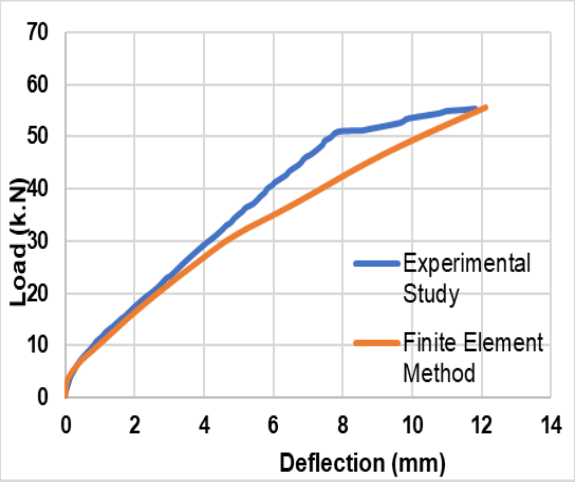

j) Load-Deflection Curves for Beam (F2).

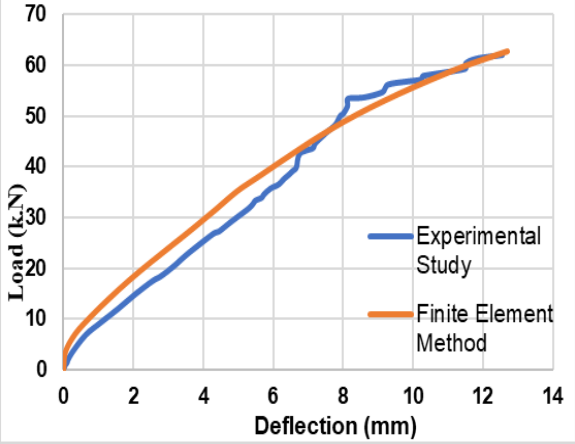

k) Load-Deflection Curves for Beam (F3).

Fig. (7) Load-deflection curve for test specimens for experimental and theoretical results.

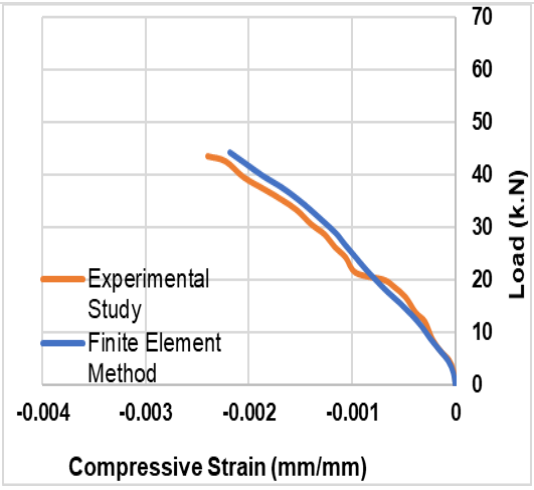

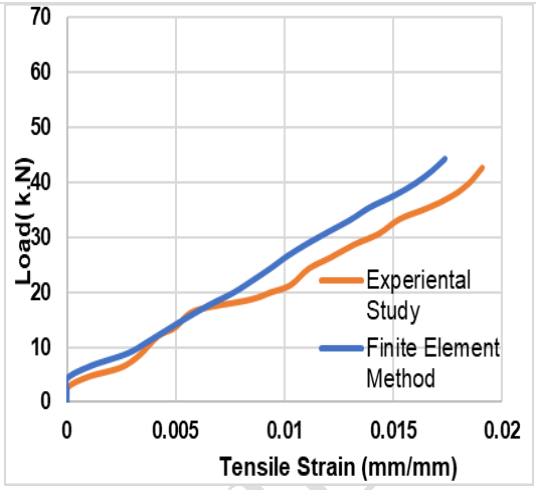

a) **Load-Compressive and Tensile Strain Curves for Beam (A1).**

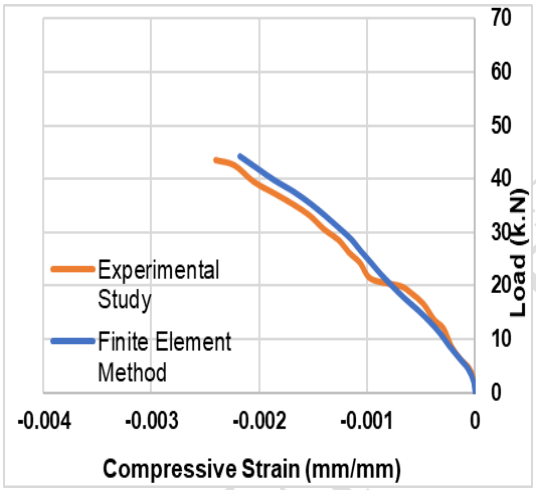

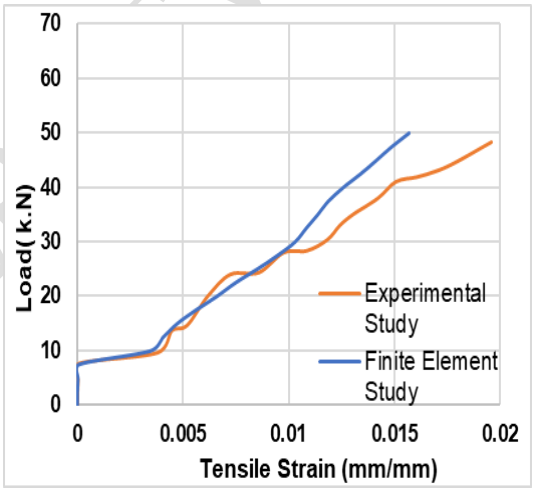

b) **Load-Compressive and Tensile Strain Curves for Beam (A2).**

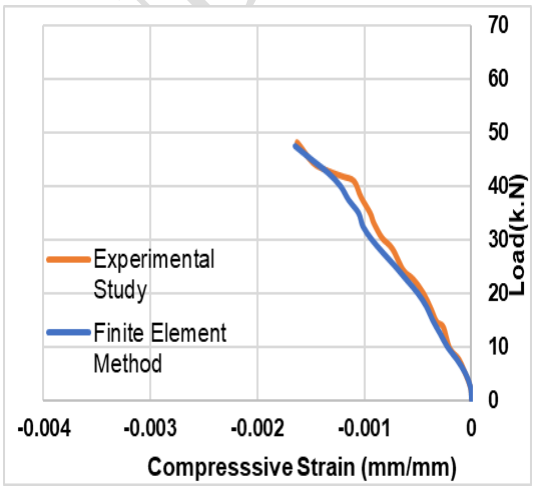

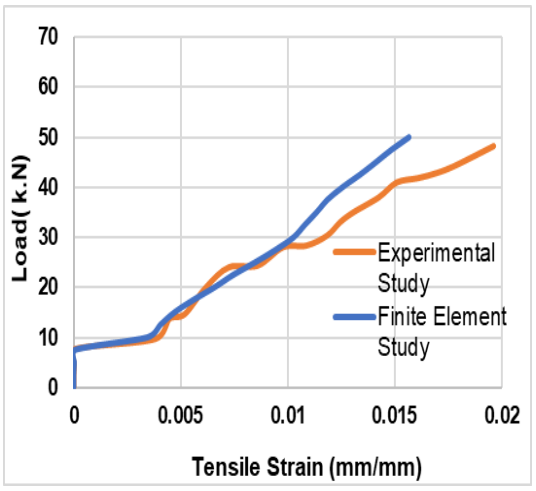

c) Load-Compressive and Tensile Strain Curves for Beam (B1).

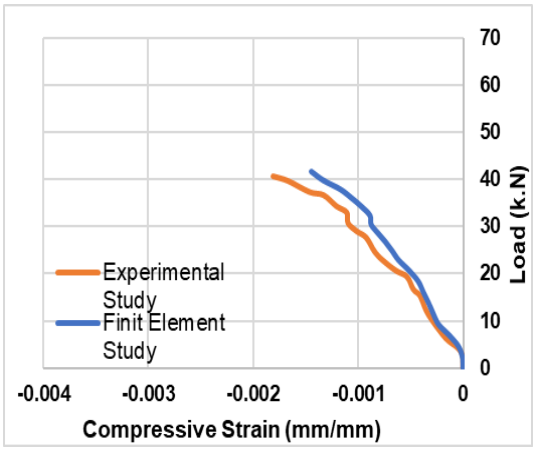

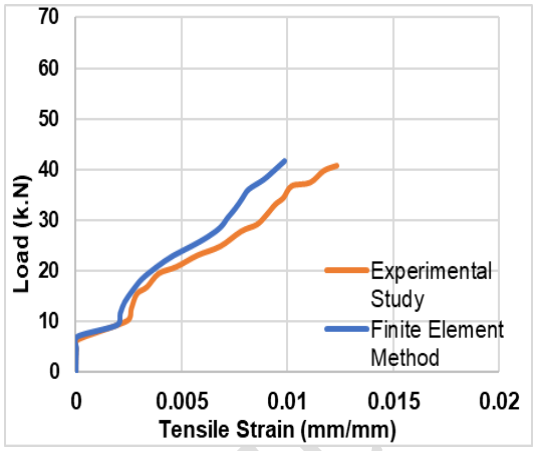

d) Load-Compressive and Tensile Strain Curves for Beam (B2).

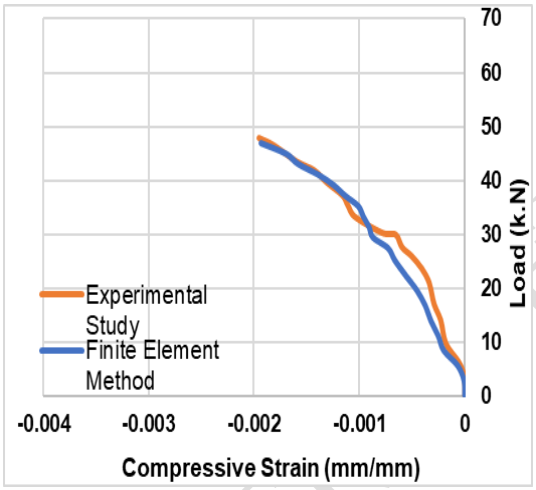

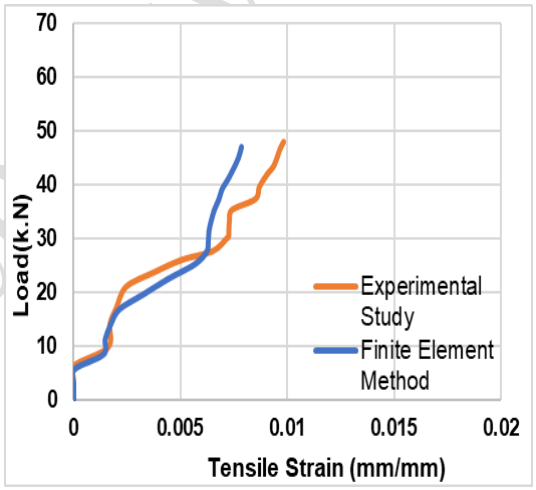

e) Load-Compressive and Tensile Strain Curves for Beam (B3).

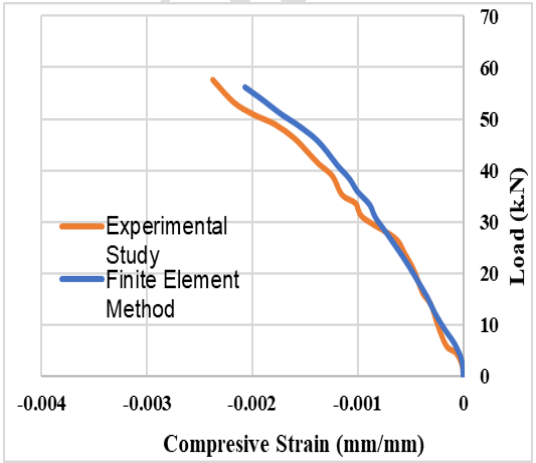

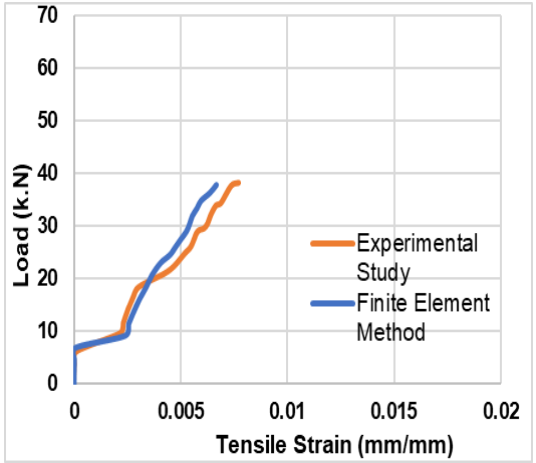

f) Load-Compressive and Tensile Strain Curves for Beam (G1).

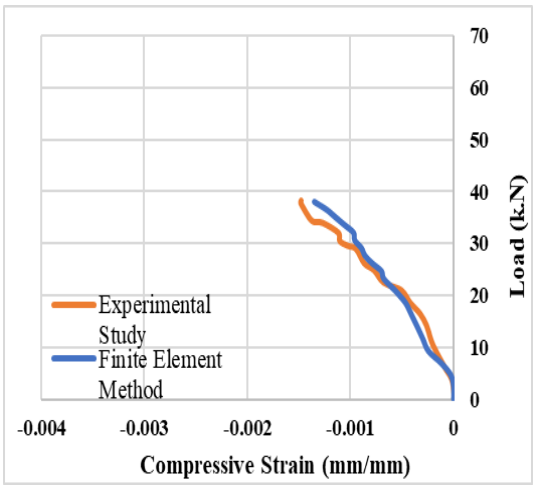

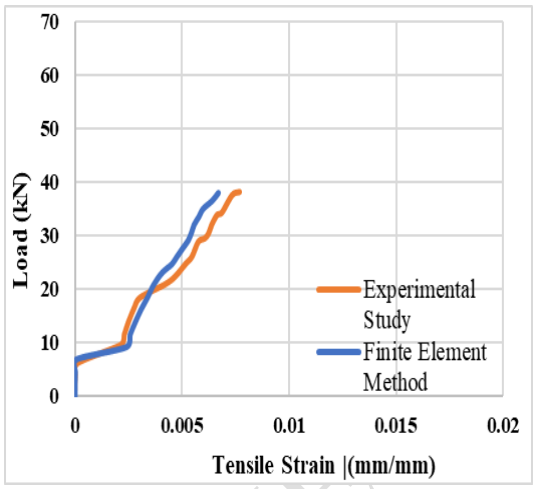

g) Load-Compressive and Tensile Strain Curves for Beam (G2).

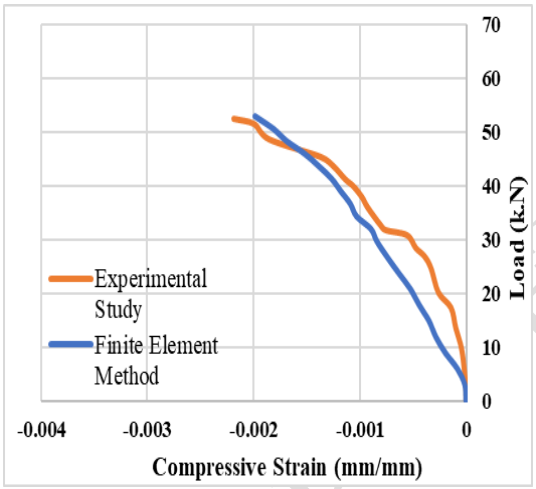

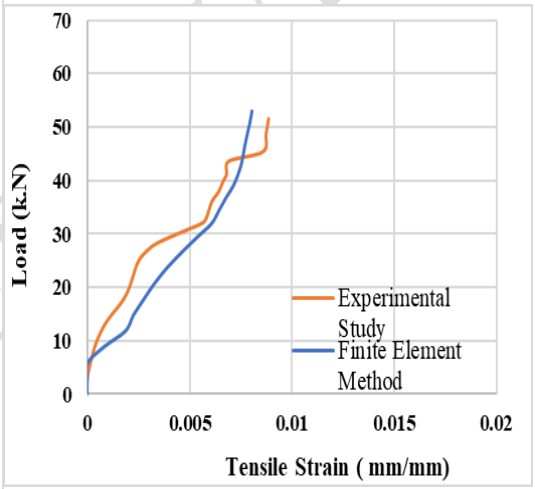

h) Load-Compressive and Tensile Strain Curves for Beam (G3).

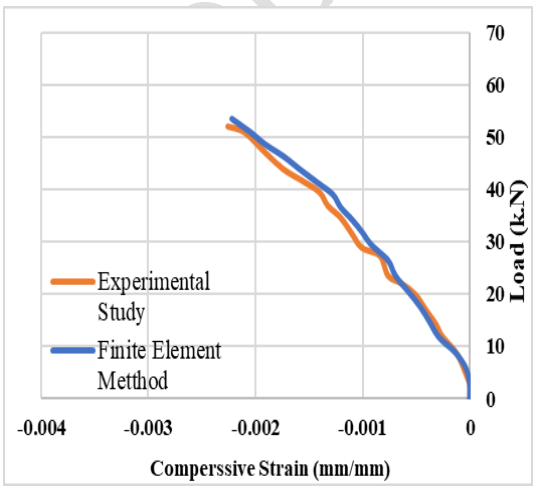

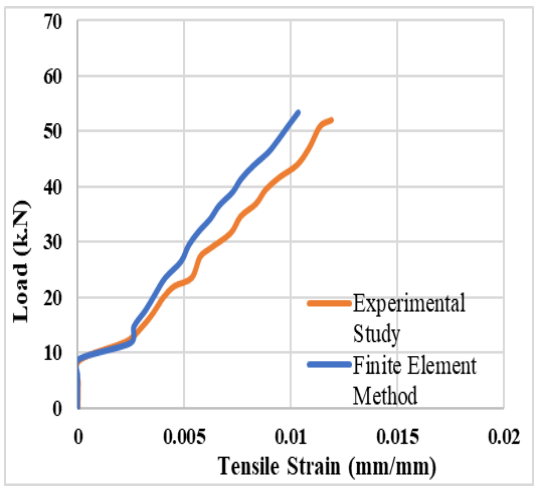

i) Load-Compressive and Tensile Strain Curves for Beam (F1).

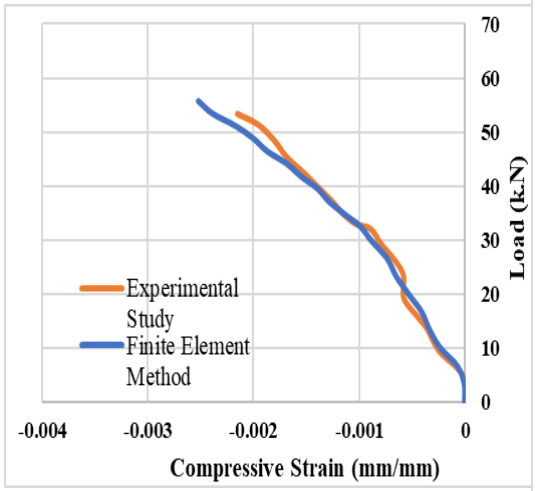

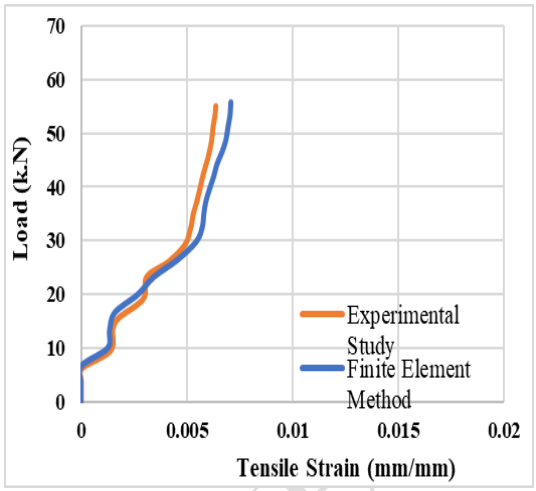

j) **Load-Compressive and Tensile Strain Curves for Beam (**F2**).**

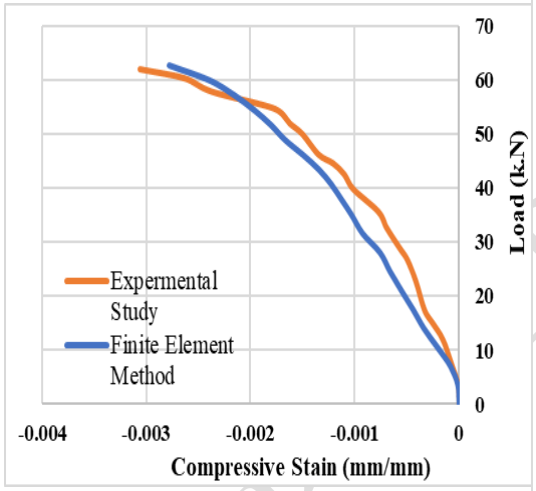

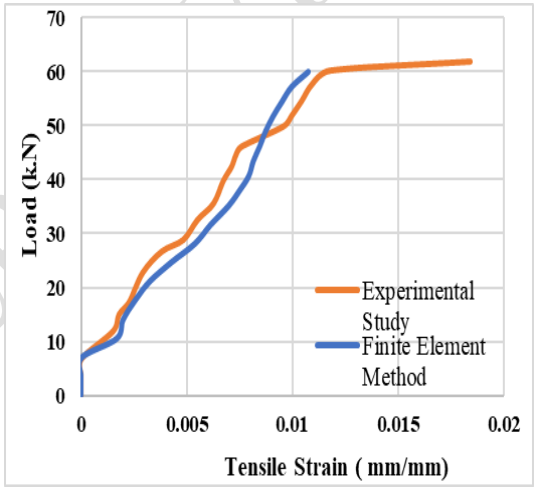

k) **Load-Compressive and Tensile Strain Curves for Beam (**F3**).**

Fig. (8) Load- Strain Curves for Beam Tested for Experimental and Theoretical Results.

4.7 COMPARSION OF CRACKING PATTERNS OF ALL TESTED BEAMS

Figures from (9) to (20) represent compression between failure modes and crack patterns of all beams tested as published and the corresponding finite element model

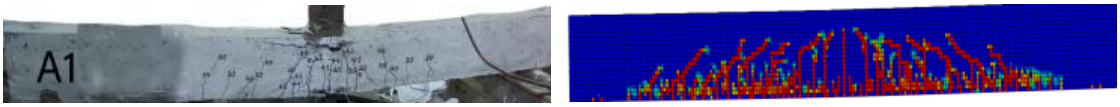

a) Cracking Patterns for Beam (A1) [EXP]. b) Cracking Patterns for Beam (A1) [FEM].

Fig. (9) Failure pattern for Beam (A1).

a) Cracking Patterns for Beam (A2) [EXP]. b) Cracking Patterns for Beam (A2) [FEM].

Fig. (10) Failure pattern for Beam (A2).

a) Cracking Patterns for Beam (B1) [EXP]. b) Cracking Patterns for Beam (B1) [FEM].

Fig. (11) Failure pattern for Beam (B1).

a) Cracking Patterns for Beam (B2) [EXP]. b) Cracking Patterns for Beam (B2) [FEM].

Fig. (12) Failure pattern for Beam (B2).

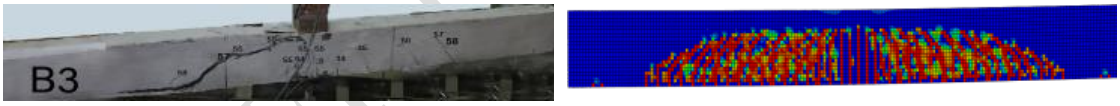

a) Cracking Patterns for Beam (B3) [EXP]. b) Cracking Patterns for Beam (B3) [FEM].

Fig. (13) Failure pattern for Beam (B3).

a) Cracking Patterns for Beam (G1) [EXP]. b) Cracking Patterns for Beam (G1) [FEM].

Fig. (14) Failure pattern for Beam (G1).

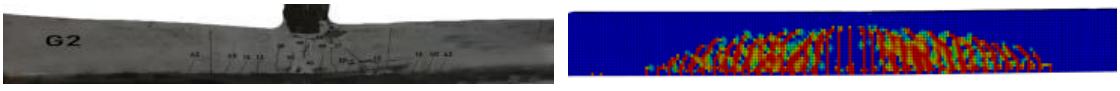

a) Cracking Patterns for Beam (G2) [EXP]. b) Cracking Patterns for Beam (G2) [FEM].

Fig. (15) Failure pattern for Beam (G2).

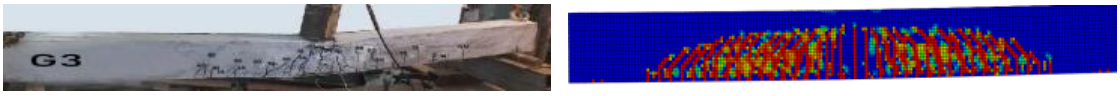

a) Cracking Patterns for Beam (G3) [EXP]. **b) Cracking Patterns for Beam (G3) [FEM].**

Fig. (16) Failure pattern for Beam (G3).

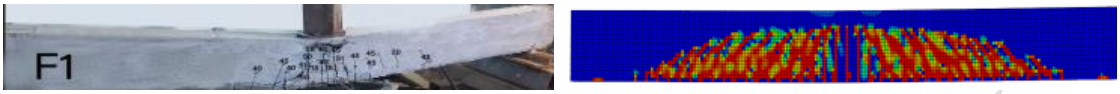

a) Cracking Patterns for Beam (F1) [EXP]. **b) Cracking Patterns for Beam (F1) [FEM].**

Fig. (17) Failure pattern for Beam (F1).

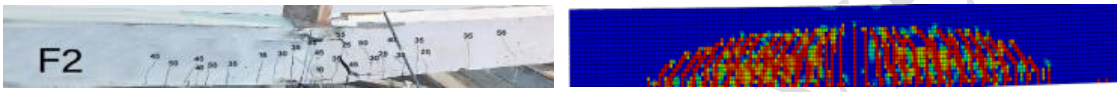

a) Cracking Patterns for Beam (F2) [EXP]. **b) Cracking Patterns for Beam (F2) [FEM].**

Fig. (18) Failure pattern for Beam (F2).

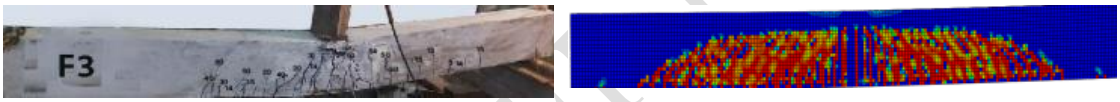

a) Cracking Patterns for Beam (F3) [EXP]. **b) Cracking Patterns for Beam (F3) [FEM].**

Fig. (19) Failure pattern for Beam (F3).

5. Conclusion

The goal of this study's experimental program was to compare the flexural behavior of lightweight ferrocement composite beams to that of traditional structural reinforced concrete beams under focused loads. The inferences that can be made are as follows:

1. The theoretical methods for first crack and ultimate load calculations provide good prediction for these loads and the beam's mode of failure.

2.The results obtained from the finite element analysis agreed well with the experimental ones for all test specimens. It could be concluded that the finite element model could be reasonably used to predict the behavior of the beam system under consideration.

.

.

REFERENCES

1.Monisha KM, Srinivasan G. Experimenta Behaviour of Prestress Hollow Core Slab, Rc Hollow Core Slab and Normal Rc Solid Slab. Int J Eng Tech Res. 2017; 4:1090–3.

2. Acma L, Dumpasan G, Salva M, Mansaguiton M, Supremo R, Daquiado N. Flexural strength and ductility behavior of ferrocement I-beam, Mindanao Journal of Science and Technology. 2015; 13:99-108.

3.Eskandari H, Madadi A. Investigation of ferrocement channels using experimental and finite element analysis. Engineering Science and Technology, an International Journal. 2015;18(4):769-775.

4.Structural Behavior of Light Weight Ferrocement Walls. 13th International Conference on Civil and Architecture Engineering. cairo, Egypt. 2020;1-21.

5.Shaaban IG, Shaheen YB, Elsayed EL, Kamal OA, Adesina PA. Flexural behaviour and theoretical prediction o lightweight ferrocement composite beams. Case studies in construction materials.2018;9.

6. Abbass AA, Abid SR, Arna'ot FH, Al-Ameri R A, Özakça M. Flexural response of hollow high strength concrete beams considering different size reductions. Journal of Structures. 2020; 23:69-86.

7.Naser FH, Al Mamoori AH, Dhahir MK (2021). Effect of using different types of reinforcement on the flexural behavior of ferrocement hollow core slabs embedding PVC pipes. Ain Shams Engineering Journal. 2021;12(1):303-315.

8.Prakashan LV, George J, Edayadiyil JB, George JM. Experimental Study on the Flexural Behavior of Hollow Core Concrete Slabs. Journal of Applied Mechanics and Materials. 2016; 857:107-112.

9.ASTM C778 Graded Sand ASTM "Cement testing standard specifications for standard sand **".**

10.Egyptian Standards Specification, E.S.S, 4756-11. (2012). Physical and mechanical properties examination of cement, part 1, Cairo.

11.ASTM C494/C 494 M. (2001). Standard specification for chemical admixtures for concrete.Annual Book of ASTM Standards, 4(2), 9.

12.Korany, Y.S. (1996) "Repairing Reinforced Concrete Columns Using Ferrocement Laminates", MS thesis submitted to The American University in Cairo, Egypt.

13. ASTM C618-19. (2019), Standard Specification for Coal Fly Ash and Raw or Calcined Natural Pozzolan for Use in Concrete, ASTM International, West Conshohocken, PA, http://www.astm.org/.

14.Data sheet of Fine Expanded Perlite from CMB.

15.Plena Egypt, Delta Sand Bricks Co "The Cost Saving Blocks", a manufacturer's catalogue.

16.https://www.cmbegypt.com/cmb/datasheets/en/pdf/12-sound-and-thermal -insulation /advefoam.pdf.

17.Yousry B. I. Shaheen, Mohammed El-Sabbwy, Dina Ahmed El-Bordeny. Structural characteristics of lightweight ferrocement beams with different core material. Journal of Engineering Research and Reports.Pub.2022/ JERR/91928.

18.Abaqus User's Guide (2013). Abaqus Documentation. User's Guide. s.l.: Dassault Systems, Simulia Corp.